Clays and Clay Minerals, Vol. 36, No. 4, 327–336, 1988.

HYDROTHERMAL ALTERATIONS OF HISINGERITE MATERIAL FROM A BASALT QUARRY NEAR GEELONG, VICTORIA, AUSTRALIA

AHMAD SHAYAN,[1] JOHN V. SANDERS,[2]
AND CHRISTOPHER J. LANCUCKI[1]

[1] CSIRO Division of Construction and Engineering, P.O. Box 56
Highett, Victoria 3190, Australia

[2] CSIRO Division of Materials Science and Technology, P.O. Box 160
Clayton, Victoria 3168, Australia

Abstract—To understand the genetic relationship between hisingerite material in the joints of an overlying grey basalt and nontronite and Fe-rich saponite in the joints and matrix of a more deuterically altered, underlying green basalt, the hisingerite material was treated in a series of hydrothermal experiments. No well-ordered clay mineral was produced at temperatures <340°C, although extended treatment for 445 days and at 110°C or 42 days at 180°C resulted in the formation of materials that gave broad, weak, basal X-ray powder diffraction (XRD) reflections characteristic of 2:1 phyllosilicates. Hematite did not form at 110°C, but it did form at 180°C in 1- and 6-week runs. Treatments at 340°C in Pt, Ag-Pd, and Au containers resulted in mixtures of Fe-rich saponite + hematite, but the same starting material treated at 340°C in stainless steel yielded, in addition, some chlorite, probably due to the more reducing conditions in the stainless steel container. Treatment of the unaltered grey basalt at 340°C and 50 MPa for 10 days resulted in complete alteration of olivine (and probably glass) to a trioctahedral smectite.

The Fe-rich saponite produced by the hydrothermal treatment of the hisingerite material has a composition and XRD pattern similar to the Fe-rich saponite found in the green basalt and an XRD pattern similar to that produced by the hydrothermal treatment of the grey basalt; thus these clays may have had a similar origin. The compositions and XRD patterns of these clays are not similar, however, to those of the nontronite in the joints of the green basalt. The nontronite probably formed during a subsequent low-temperature alteration.

Key Words—Basalt, Deuteric alteration, Hisingerite, Hydrothermal treatment, Nontronite, Saponite.

INTRODUCTION

Three basalt flows have been exposed in a basalt quarry near Geelong, Victoria, Australia (Figure 1) as a result of quarrying operations. An uppermost, weathered grey basalt (third flow) and a middle, highly altered black basalt (second flow) are removed as overburden for access to a grey, slightly deuterically altered basalt (first flow), which is used as a high-quality construction material. The first-flow lava, about 25 m thick, flowed into a river gully (Coulson, 1977), which contained a sediment consisting of smectite, mica, and quartz. The resulting steam appears to have deuterically altered the lower part of the flow (about 8–10 m) and produced a color change from grey to green. Such a color change in a comparable flow in another basalt quarry has been attributed to deuteric alteration of glass and olivine to saponitic and nontronitic clay minerals (Cole and Lancucki, 1976).

Hisingerite material has been reported in joints in the grey, first-flow basalt (Shayan, 1984). The green, altered part of this grey basalt contains iron-rich saponite in the matrix and nontronite and goethite in joints. The apparently more intense deuteric alteration of the lower part of this flow was probably due to its contact with the steam generated from the river bed when the lava flowed into the river. The hisingerite in the upper part of this flow and the saponite and nontronite in the lower part of this flow may have had a common genesis, the different mineral assemblages reflecting only a difference in intensity and/or duration of the deuteric alteration.

To understand the possible genetic relationship between the hisingerite in the joints of the upper part of this flow and the nontronite and saponite in the lower part, samples of the hisingerite and the grey basalt were subjected to laboratory hydrothermal treatment between 100° and 400°C.

BACKGROUND

Clay minerals in altered subaerial basalts range from Fe-rich saponite and nontronitic (Cole and Lancucki, 1976) to swelling chlorite (Bain and Russell, 1981), Fe-rich smectite (Walters and Ineson, 1983), and Fe-rich saponite and subsidiary interstratified chlorite (Cowking *et al.*, 1983). These Fe-rich smectites apparently formed from interstitial glass and olivine (Cole and Lancucki, 1976; Walters and Ineson, 1983) in the mildly (deuterically or hydrothermally) altered basalts. During intensive weathering, where plagioclase also altered, the Fe-poor, Al-rich dioctahedral clay minerals, montmorillonite, vermiculite, and illite, form in basalt rubble, and the Fe-rich varieties are destroyed

Copyright © 1988, The Clay Minerals Society

https://doi.org/10.1346/CCMN.1988.0360406 Published online by Cambridge University Press

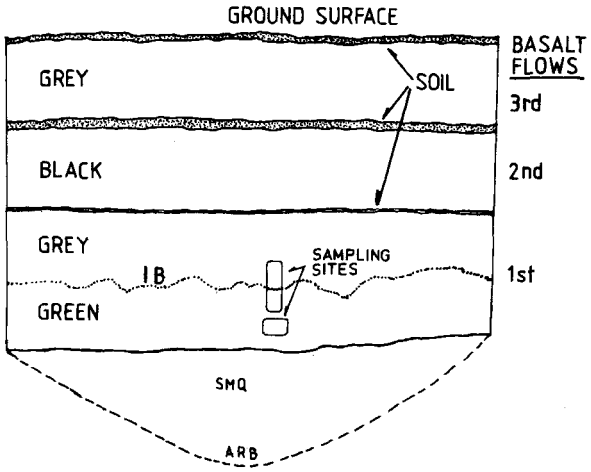

Figure 1. Schematic representation (not to scale) of the basalt flows exposed at the quarry near Geelong. Soil layers indicate some weathering of the underlying basalts. IB = irregular boundary, ARB = ancient river bed, SMQ = smectite-, mica-, and quartz-bearing sediment. No evidence exists for weathering of the green basalt of the first flow.

(Bain and Russell, 1980; Bain *et al.*, 1980). Eggleton *et al.* (1987) found that whereas weathered rinds of basalts from eastern Australia are dominated by halloysite and goethite, the much less weathered, hard core-stones are dominated by smectite. Unlike the weathered shallow rocks examined by Eggleton *et al.* (1987), the green and grey basalt samples studied here do not appear to have undergone appreciable aerial weathering subsequent to their placement. The presence of Fe-rich saponite and nontronite in the green basalt from Geelong, thus, indicate a mild alteration (deuteric). The presence of hisingerite rather than clay minerals in the joints of the grey basalt (Shayan, 1984) indicates a much less severe alteration.

The reaction of basalt lava and seawater also produces Fe-rich saponite and nontronite (Scheiddegger and Stokes, 1977). Papavassiliou and Cosgrove (1981) found that the upper regions of ocean-floor basalt contained dioctahedral Fe^{3+}-rich smectite and Fe^{3+} oxide/hydroxide, whereas the deeper regions contained trioctahedral smectite and smectite/chlorite mixed-layer minerals. Thus, the oxidation/reduction potential influenced the type of clay formed during basalt alteration. These authors also indicated that the source of the clay minerals in the altered submarine basalts was glass, olivine, and, to a lesser extent, pyroxene, although alteration of feldspars must have provided the Al contained in the alteration clay. Seyfried *et al.* (1976), Noack *et al.* (1979), and many other researchers involved with the Deep Sea Drilling Project reported Fe- and Mg-rich smectites in altered submarine basalts. The clay mineralogies of deuterically altered subaerial and submarine basalts, thus, appear to be similar.

A study of the alteration of submarine basaltic lavas (Scott and Hajash, 1976) and the experimental investigations of hydrothermal reactions between basaltic glass, and basalt, and seawater or synthetic salt solutions (Bischoff and Dickson, 1975; Hajash, 1975; Mottl and Holland, 1978; Seyfried and Bischoff, 1979, 1981) have provided valuable information on the processes of alteration of submarine basalt. In these processes Mg^{2+} and SO_4^{2-} always appear to have been removed from seawater and retained by the alteration minerals, including clay minerals, anhydrite, and some sulfides. Cations, such as Ca, Na, K and Si, were generally released into solution initially, but precipitated later as solid phases, depending on the experimental conditions, such as temperature, solution composition, solution/rock ratio, and time. The direction of ion exchange of basalt with seawater evidently reverses, particularly for Mg and Na, during the subsequent low-temperature reaction. Thus, Fe-rich saponite may lose Mg during low-temperature alteration and transform to nontronite. In these experiments basalt glass and olivine were found to be least resistant to alteration, followed by pyroxene; the most resistant phase was plagioclase.

In view of the mineralogical similarities between clay minerals produced in these hydrothermal experiments and those resulting from natural alteration of basalts, the hisingerite material and the grey basalt were subjected to hydrothermal treatment. The similarity of the resulting clay minerals to the natural products formed in the altered green basalt suggest that the components that alter to the same clay mineral had a similar origin.

EXPERIMENTAL

Starting materials

The starting material for all hydrothermal runs, except one, was the hisingerite material described by Shayan (1984). The material which coated some joint surfaces of the grey basalt was separated with a blade, hand-picked under a stereoscopic microscope, and ground to <75 μm particle size. The final powdered sample contained a trace of siderite and pyrite impurities; its chemical composition is given in Table 1.

A powder sample (<75 μm) of the unaltered grey basalt was used for one hydrothermal run (see below). The chemical composition of the basalt determined by X-ray fluorescence is also given in Table 1. It consisted of olivine phenocrysts, an ophitic matrix of pyroxene and feldspar, and dark glass containing magnetite needles.

Hydrothermal treatment

Hydrothermal treatments were carried out on 200–300 mg of powder or hand-pressed pellets as follows: (1) powder samples were placed in small Pt crucibles or sealed with 70 mg of distilled water in Ag-Pd capsules and treated at 180°C and 1.7 MPa in an autoclave

https://doi.org/10.1346/CCMN.1988.0360406 Published online by Cambridge University Press

Table 1. Composition (wt. %) of the starting materials for the hydrothermal runs.

	Hisingerite[1]	Grey basalt
SiO_2	34.20	51.12
TiO_2	0.28	1.97
Al_2O_3	4.16	14.10
Fe_2O_3	17.10	10.22[2]
FeO	4.15	
MnO	0.08	0.14
MgO	5.70	7.17
CaO	0.91	8.24
Na_2O	0.67	3.54
K_2O	0.26	1.16
P_2O_5	0.05	0.38
H_2O+	5.30	
H_2O-	25.40	0.41[3]
CO_2	1.23	
Total	99.49	99.00

[1] Taken from Shayan (1984).
[2] Total Fe given as Fe_2O_3.
[3] Loss on ignition.

for 1 day, 1 week, and, for one sample, in a Pt crucible for 6 weeks; (2) powder samples + 100 mg of distilled water were placed in 5-cm^3 stainless steel containers and treated at 340°C and 13.8 MPa for 1 day and 1 week; those in Pt and Ag-Pd capsules were treated for 1 week; (3) powder samples + 70 mg water were placed in sealed Ag-Pd capsules and pellets were placed in unsealed Pt foil and treated at 370°C and 13.8 MPa for 1 day and 1 week; (4) powder samples + 70 mg water were sealed in Au and Ag-Pd capsules, either alone or encapsulated with Co-CoO buffer in another Au capsule and treated at 370°C and 50 MPa for 1 week; (5) powder samples (2 g) + 5 mg water were placed in a 50-cm^3 stainless steel container and heated in an oven at 110°C for as long as 445 days; and (6) a powder sample (100 mg) of the grey basalt from the first flow + 70 mg water were placed in a sealed Ag-Pd container and treated at 340°C and 50 MPa for 10 days.

Analyses

After each treatment X-ray powder diffraction (XRD) patterns were taken with a Philips PW1050/81 powder diffractometer and monochromatic CuKα radiation (30 kV, 15 mA, scanning rate of 0.5°2θ/min). XRD patterns were also obtained for (1) oriented air-dried samples, (2) samples treated with glycerol or dimethylsulfoxide (DMSO), and (3) samples heated at 580°C for 1 hr. Infrared (IR) spectra were obtained on a Perkin-Elmer 1430 ratio-recording instrument using 0.5- or 1.0-mg samples in 200-mg KBr disks. Differential thermal (DTA) and thermogravimetric (TGA) analyses were made simultaneously on a Stanton Redcroft ST781 analyzer using 10-mg samples and a heating rate of 10°C/min. A Cambridge scanning electron microscope (SEM) equipped with an energy-dispersive X-ray spectrometer (EDX) was used to indicate, from an examination of compositions, if minor phases were produced by the treatments. The product of the treatment at 370°C, which contained hematite + Fe-rich saponite, was treated with dithionite-citrate-bicarbonate (DCB) to purify the Fe-rich saponite by removing free iron oxides (Mehra and Jackson, 1960). The purified material was hand-pressed into a flake and analyzed in an ARL-EMX electron microprobe equipped with an EDX system and operated at 15 kV and a 1-nA beam current. A JEOL 100 CX transmission electron microscope (TEM) was used to determine the morphological features of various samples. This instrument was equipped with an attachment that allowed specimens to be examined before and after heating in vacuum or in hydrogen, without contacting the specimen with air.

RESULTS AND DISCUSSION

X-ray powder diffraction analysis

XRD patterns of the treated samples are shown in Figure 2. Trace 1 represents both the untreated hisingerite material and the material treated for 1 day at 180°C. The treatment had no effect except that the color changed from grey green to red brown. The same treatment for one week in various containers, however, resulted in the formation of small amounts of hematite (trace 2). After 6 weeks, more hematite and weak basal reflections of 2:1 layer phyllosilicates were also evident, similar to those shown in trace 3. Treatments for 1 day at 340° and 370°C (trace 3) produced larger amounts of hematite. In addition, the low-angle region of the XRD traces suggests that some 2:1 layer clay minerals also formed. The reflection at 3.50 Å may be due to small amounts of anhydrite, which formed from the trace of pyrite impurity in the original sample and Ca from the hisingerite. Anhydrite is a common hydrothermal product of materials similar to those investigated here (Hajash, 1975; Seyfried *et al.*, 1976; Mottl and Holland, 1978).

The treatments at 340°C in stainless steel containers (trace 4) produced hematite, smectite, and chlorite, whereas the same treatment in the Pt and Ag-Pd containers produced hematite and smectite only. The latter assemblage was also produced in runs at 370°C in the various containers with or without Co-CoO buffer (trace 5), although more hematite was produced at the higher temperature. From its 060 reflection at 1.537 Å (i.e., trioctahedral) and its Mg- and Fe-rich nature (Table 2), this smectite was probably an Fe-rich saponite.

The formation of chlorite appears to have been related to the use of stainless steel as a container, because chlorite did not form in runs made in other types of containers under similar conditions. A more reducing condition probably prevailed in the stainless steel container; from standard tables of redox potential it is

https://doi.org/10.1346/CCMN.1988.0360406 Published online by Cambridge University Press

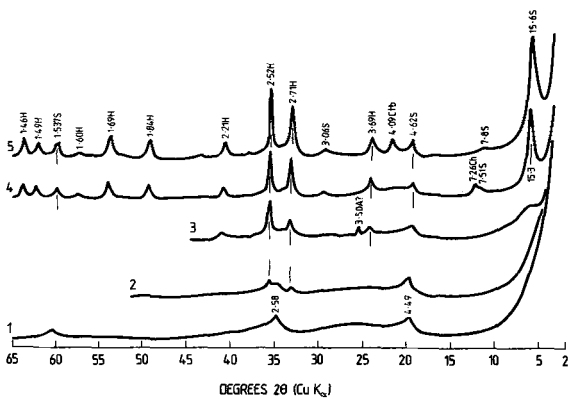

Figure 2. X-ray powder diffraction patterns of: (1) hisingerite material untreated (same as that treated at 180°C for 1 day); (2) treated for 1 week at 180°C; (3) treated for 1 day at 340°C or 370°C; (4) treated for 1 week at 340°C in stainless steel container; and (5) treated for 1 week at 370°C in platinum, silver-palladium, or gold containers. S = saponite, H = hematite, Ctb = cristobalite, Ch = chlorite, A? = possibly anhydrite. Spacings are given in Å.

evident that Fe is a much stronger reducer than Au, Ag, or Pt. From the XRD patterns (Figure 2), hematite clearly formed prior to the formation of clay minerals from hisingerite. After the available oxygen was consumed by the formation of hematite, iron, in excess of that incorporated in the structure of the Fe-rich saponite, was probably present as Fe^{2+} and was available for the formation of the chlorite phase. As discussed below, chlorite and magnetite formed under the reducing conditions in the center of a thick hisingerite pellet, whereas smectite (Fe-rich saponite) and hematite formed in the oxidized outer parts of the pellet that was subjected to treatment at 370°C for 1 week (*vide infra*). Senkayi *et al.* (1983) also reported that, during the weathering of lignite overburden, the oxidized zone was characterized by the presence of reddish brown, crystalline iron oxide and by the absence of chlorite, whereas chlorite was present in the reduced zone. Papavassiliou and Cosgrove (1981), also indicated that chlorite forms under more reducing conditions than are required for the formation of Fe^{3+}-rich smectites.

The difference between the runs at 340°C in stainless steel and those at 370°C in other types of containers is more clearly shown in the XRD patterns of oriented samples in Figure 3. Because the 002 reflection of chlorite (7.2 Å) is much more intense than the 001 reflection (14.2 Å), the chlorite is probably Fe-rich (Brindley, 1972). The 001 reflection of chlorite is masked in the XRD trace of the air-dry sample by the strong 001 reflection of Fe-rich saponite, and it is extremely weak in the trace of the DMSO-treated product because a general loss in intensity occurs for glycerol- and DMSO-treated samples (cf. peak intensities in the traces of the air-dry and DMSO-treated samples). Heating the sample at 580°C collapsed the (001) spacing of Fe-rich saponite to about 10 Å and destroyed the 002 reflection of chlorite and enhanced its 001 reflection. The reflection at 7.2 Å in the trace of the air-dry product is probably not due to kaolinite, because the DMSO treatment produced no reflection at 11.2 Å. The treatment with dithionite-citrate-bicarbonate (Mehra and Jackson, 1960) removed about 20% hematite from the Fe-rich saponite-hematite mixture, which was produced by the treatment at 370°C (Figure 2), and the XRD

Table 2. Electron microprobe analysis[1] and recalculated composition[2] of purified saponite.

	Wt. %	Atoms[3]			Atoms[4]		
SiO_2	48.28 (1.23)	Si	6.89	8.0	Si	7.11	8.0
TiO_2	0.20 (0.08)	Al	0.95		Al	0.89	
Al_2O_3	5.66 (2.40)	Fe^{3+}	0.16				
Fe_2O_3	12.71 (1.53)						
or[5]	or						
FeO	11.44						
MnO	0.35 (0.26)	Fe^{3+}	1.21	5.56	Al	0.10	6.00
MgO	20.16 (3.99)	Ti	0.02		Fe^{2+}	1.41	
CaO	0.13 (0.21)	Mn	0.04		Ti	0.02	
Na_2O	2.34 (0.66)	Mg	4.29		Mn	0.04	
					Mg	4.43	
K_2O	0.19 (0.17)	Ca	0.02	0.70	Ca	0.02	0.73
Subtotal	90.02	Na	0.65		Na	0.67	
H_2O[6]	9.82	K	0.03		K	0.04	
Total	99.84						

[1] Average of 8 analyses. Standard deviations are given in parantheses.
[2] On the basis of 22 oxygens.
[3] Atom proportions if total iron is calculated as Fe^{3+}.
[4] Atom proportions if total iron is calculated as Fe^{2+}.
[5] Total Fe is calculated either as Fe_2O_3 or as FeO.
[6] Total water content determined on a 2-mg sample by the Australian Mineral Development Laboratories, using microanalytical techniques for H determination.

https://doi.org/10.1346/CCMN.1988.0360406 Published online by Cambridge University Press

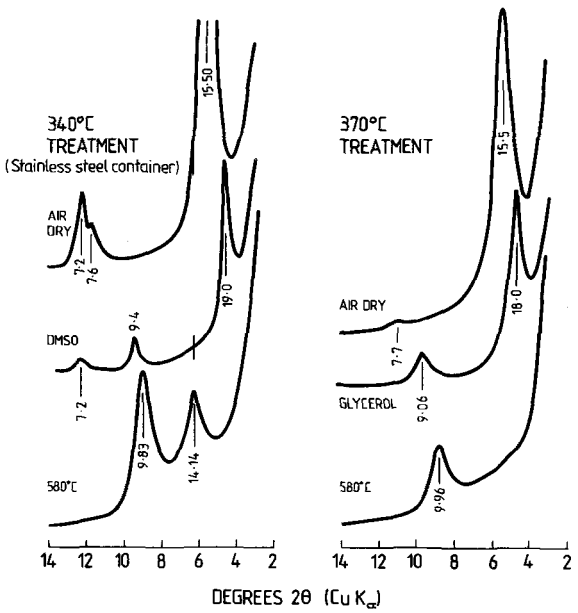

Figure 3. X-ray powder diffraction patterns of oriented samples of the products of hydrothermally treated hisingerite. The 370°C treatment yielded saponite, but both saponite and chlorite formed in the 340°C treatment in stainless steel container. DMSO = treated with dimethysulfoxide, S = saponite, Ch = chlorite. Spacings are given in Å.

pattern of the residue showed no reflections of hematite.

To supplement the relatively short runs described above, a slurry of hisingerite (2 g) in H_2O (5 ml) was treated at 110°C for as long as 445 days in a stainless steel container. In addition to anhydrite, the XRD pattern of the product showed weak, broad reflections in the low-angle region, indicative of poorly ordered 2:1 phyllosilicates. Unlike the short runs described above, no crystalline iron oxide formed; iron, therefore, was apparently not released from hisingerite in the runs made at 110°C.

Treatment of the unaltered grey basalt at 340°C and 50 MPa for 10 days resulted in the complete alteration of olivine (and probably glass) to a trioctahedral smectite having an XRD pattern similar to that of the Fe-rich saponite. Pyroxene and feldspar may have partially altered to smectite, because their reflections in the XRD patterns of the treated samples were weaker than those in the XRD pattern of the untreated grey basalt.

The formation of smectite at the expense of olivine (and probably glass) in the grey basalt indicates that the absence of clay minerals in the grey basalt is probably related to the lack of deuteric alterations. The persistence of hisingerite in the grey basalt, compared with the clay minerals in the green basalt, may also be due to the same reason.

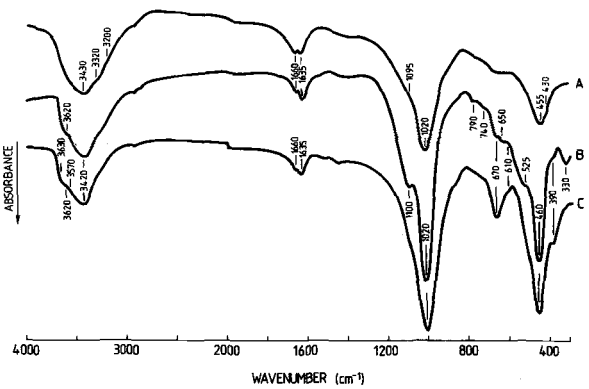

Figure 4. Infrared spectra of: (A) untreated hisingerite material, (B) hisingerite material treated at 370°C for one week, i.e., a mixture of hematite and saponite; and (C) sample B extracted three times with dithionite-citrate-bicarbonate to remove hematite. Run (A) = 0.5 mg sample, runs (B) and (C) = 1.0 mg sample/200 mg KBr.

Infrared spectroscopic analysis

The IR spectra of the untreated hisingerite material, of that treated at 370°C for 1 week (i.e., a mixture of Fe-rich saponite and hematite, *vide supra*), and of the latter product after removal of hematite by the DCB treatment are shown in Figure 4. Whereas the spectrum of the original hisingerite (Figure 4A) shows OH vibrations due to structurally bonded water molecules only (1635, 1660, and 3200–3430 cm^{-1}), the spectrum of the hydrothermally treated material (Figure 4B) shows OH-stretching vibrations due to Mg/Fe^{2+}-OH of the saponite in the region 3570 to 3630 cm^{-1}. The absorption band at 1100 cm^{-1} in spectrum B is probably due to hematite or the product of its interaction with Fe-rich saponite, because the band was absent after hematite had been removed from the sample (Figure 4C). The absorption bands at 330, 525, and 650 cm^{-1} are due to hematite (Van der Marel and Beutelspacher, 1976). The band at 670 cm^{-1} (Si–O–Mg vibrations) was more pronounced after hydrothermal treatment of the sample and the removal of hematite, suggesting a greater structural organization relative to the original hisingerite material. The Si–O–Si vibration at 1020 cm^{-1} and the Si–O and/or Mg–O vibrations

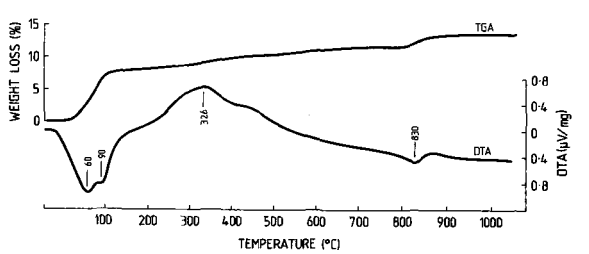

Figure 5. Differential thermal analysis and thermogravimetric analysis curves of purified saponite, corresponding to sample yielding spectra (C) in Figure 4.

https://doi.org/10.1346/CCMN.1988.0360406 Published online by Cambridge University Press

Figure 6. Transmission electron micrograph of untreated hisingerite material.

at about 460 cm^{-1} are common to all the spectra. The spectrum of the Fe-rich saponite purified by the CDB treatment of Mehra and Jackson (1960) (Figure 4C) differs slightly in the position of bands from some of the published spectra for saponite (Post, 1984; Van der Marel and Beutelspacher, 1976), possibly due to compositional differences as indicated by the latter authors. The IR spectra strongly suggest that the hydrothermal treatment resulted in the introduction of OH ions into and the removal of Fe from the structure of hisingerite.

Differential thermal and thermogravimetric analyses

DTA and TGA curves for the original hisingerite material were reported by Shayan (1984). Figure 5 shows the DTA and TGA curves for the Fe-rich saponite produced by the treatment of the hisingerite material at 370°C. The accompanying hematite was removed by DCB treatment before the DTA and TGA run. The endothermic peaks at 60° and 90°C are due to the loss of adsorbed water, and the peak at 830°C indicates a dehydroxylation reaction. The original hisingerite material contained no OH ions; therefore, OH ions must have been incorporated into the structure during the hydrothermal treatment, which produced an ordered structure (i.e., Fe-rich saponite). The exothermic hump near 326°C in the DTA curve of the DCB-treated sample was absent in the DTA curve of another run in which the hematite had not been removed from the Fe-rich saponite. As much as 80% of structural iron in Fe-rich smectites like nontronite can be reduced to Fe^{2+} by the DCB treatment (Russell *et al.*, 1979); hence, the weak exothermic reaction at about 326°C was probably due to the oxidation of Fe^{2+} of the DCB-treated, reduced sample to Fe^{3+}. A gradual weight loss similar to that noted for this sample in the temperature range 300–830°C was also observed for an Fe-rich saponite by Kohyama *et al.* (1973) and may represent the loss of loosely held surface hydroxyls, whereas the more tightly held hydroxyls in the clay structure were lost at the higher temperature (830°C).

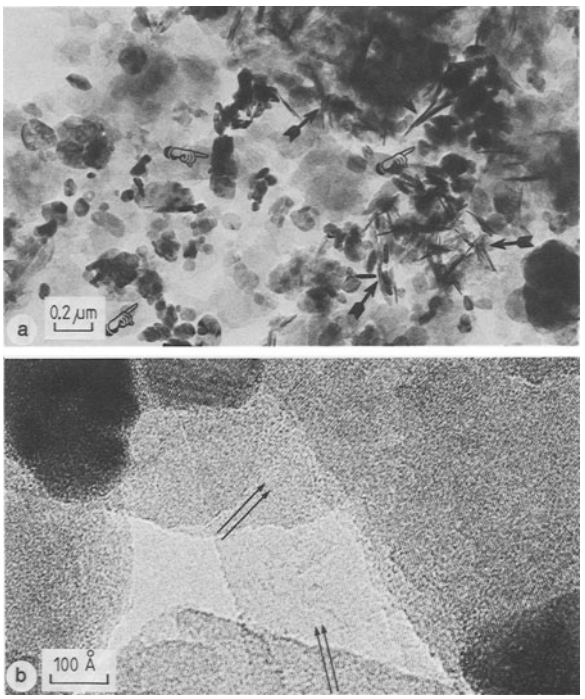

Figure 7. (A) Transmission electron micrograph of hisingerite material, after hydrothermal treatment at 370°C. Arrows show curled edges of saponite sheets, and hands point to hematite particles. (B) Higher magnification of saponite sheets showing lattice image and ordered structure. Arrows show direction of the fringes.

Electron microscopy

Hydrothermal treatment at 110° and 180°C did not significantly alter the morphology of the hisingerite material, which, as shown in Figure 6, consists of irregularly shaped and spherical bodies. The treatment at 110°C for 72 days and at 180°C for 6 weeks, however, caused a partial or full unfolding of some of the spherical bodies. This unfolding may have been responsible for the weak basal reflections in the XRD patterns of these products. Hematite particles were observed in the products of 1-day treatments at 340° and 370°C; however, irregularly shaped bodies were also present. After a 1-week treatment at these temperatures large amounts of hematite were noted in the sample, as shown in Figure 7A for the 370°C treatment. Here, curled and folded edges of the Fe-rich saponite sheets (arrows) and hematite particles (hands) can be seen. After a 1-week treatment at 340°C some of the original hisingerite material remained, as judged by the presence of the spherical bodies. The lattice-fringe image of the Fe-rich saponite sheets shows ordered structures (Figure 7B). TEMs also showed that the hematite component of the hydrothermally treated samples was effectively removed by the DCB treatment. Heating the hisingerite material in the TEM chamber in a hydrogen atmosphere or in vacuum between 300° and 600°C pro-

https://doi.org/10.1346/CCMN.1988.0360406 Published online by Cambridge University Press

duced particles <200 Å in size (Figure 8A), which were identified by electron diffraction as γ-Fe. The morphology of the original hisingerite material was preserved, as shown in Figure 8B; however, the color of the hisingerite material changed to dark brown on heating in air at such temperatures, probably due to the oxidation of structural Fe. TEM showed no evidence of either crystalline or noncrystalline iron oxide in the air-heated samples.

Electron microprobe analysis

The average of eight EMP analyses of the purified Fe-rich saponite, together with two possible structural formulae calculated on the basis of 22 oxygens, are given in Table 2. In one formula, total Fe is taken as Fe^{3+} and in the other, as Fe^{2+}. In the first formula, all of the 0.95 Al and 0.16 Fe^{3+} cations were allotted to tetrahedral positions. In view of the extensive washing of these samples with the Na-rich reagents, the exchange sites are most likely saturated with Na, as seen in Table 2. Therefore, no exchangeable Mg was allowed, resulting in an octahedral occupancy of 5.56 of 6 positions and a calculated cation-exchange capacity (CEC) of about 87 meq/100 g. Although some Fe^{3+} is possible in tetrahedral positions (e.g., Kohyama *et al.,* 1973; Cowking *et al.,* 1983), the amount shown in the recalculated formula of the present sample may be due to the dissolution of some Si and Al during the DCB treatment (Stucki *et al.,* 1984). If the total iron content was taken as Fe^{2+}, there was no need to assign Fe to the tetrahedral positions, and the occupancy of the octahedral sites became complete (i.e., 6). The resulting calculated CEC value was then 92 meq/100 g.

Despite the fact that the second formula appears to give a more reasonable approximation of the structural formula of the Fe-rich saponite, all of the Fe probably does not exist in the mineral as Fe^{2+}. The material changed from deep greenish blue to grey and finally to light brown after the DCB treatment, indicating some oxidation of iron. According to Stucki *et al.* (1984), oxidation of Fe cannot be avoided in the traditional DCB treatment, which was used in this study. Moreover, from the 060 reflections at 1.537 Å, the *b* dimension of 9.22 Å is close to that of the oxidized Fe-rich saponites reported by Kohyama *et al.* (1973). Thus, the structural formula of the Fe-rich saponite appears to be between the two given in Table 2, probably closer to the oxidized form, i.e., $(Ca_{0.02}Na_{0.65}K_{0.03})(Fe^{3+}_{1.21} \cdot Mg_{4.29}Ti_{0.02}Mn_{0.04})(Si_{6.89}Al_{0.95}Fe^{3+}_{0.16})O_{20}(OH)_4$. Structural water calculated from the TGA weight loss >300°C is 4.7% of the sample, in agreement with that contained in the above formula (4.4%).

Phases produced in the cores of hydrothermally treated thick pellet samples

Although the hydrothermal reaction products of the powdered hisingerite or thin pellets (1 mm) of the hisingerite material at 370°C were hematite + Fe-rich saponite, only the outer parts of thick pellets (~3 mm) transformed to these minerals. The core of the thick pellet was black and contained magnetite as the major component, together with minor amounts of chlorite

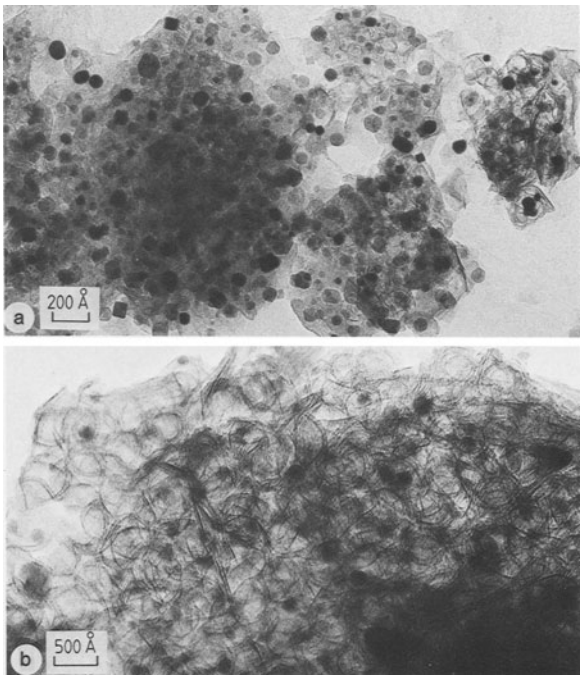

Figure 8. (A) Transmission electron micrograph of hisingerite material heated in a hydrogen atmosphere between 300° and 600°C and showing the released γ-Fe particles. (B) Higher magnification showing unchanged morphology of hisingerite material.

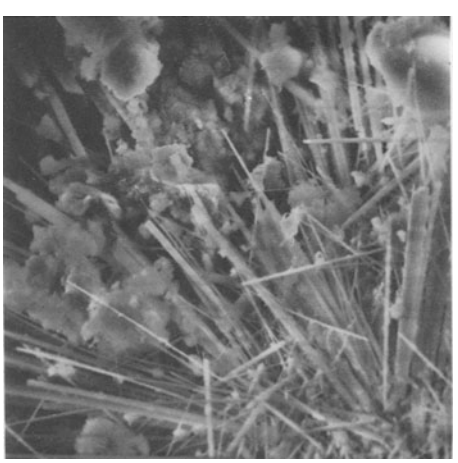

Figure 9. Acicular crystals of xonotlite formed on the surface of a thick pellet (~3 mm) of hisingerite material after treatment at 370°C and 13.8 MPa water vapor pressure for one week.

https://doi.org/10.1346/CCMN.1988.0360406 Published online by Cambridge University Press

and brucite. In addition, a weak reflection at 3.03 Å was noted in the XRD pattern of the core material corresponding to either calcite or a calcium silicate hydrate. An SEM of a faint white stain on the surface of the thick pellet showed it to consist of acicular crystals (Figure 9), and EDX indicated only Ca and Si in these crystals. An XRD film pattern, taken with a Unicam camera, showed that the crystals were xonotlite (JCPDS Card 29-379). Formation of xonotlite under temperature and pressure conditions similar to those employed in this work has been reported (Luke *et al.*, 1981; Stevula and Petrovic, 1983). The small amount of Ca present in the hisingerite (0.91% CaO) restricted the formation of xonotlite in the pellet. The presence of magnetite, rather than hematite, indicates reducing conditions in the core of the pellet; the chlorite appears to have formed under these reducing conditions, where iron was available as Fe^{2+}. The existence of brucite as a separate phase suggests alkaline conditions in the core of the pellet.

Relationship between natural and synthesized materials

Because iron (17.1% Fe_2O_3 and 3.5% FeO) and silica (34.2% SiO_2) comprise about 80% of the dry mass of the hisingerite material, hydrothermal treatment should have produced nontronite, which would partly have explained the existence of nontronite in the joints of the green basalt. Fe-rich saponite, however, formed, and most of the iron contained in the hisingerite was transformed to hematite. Minor amounts of cristobalite and anhydrite also formed.

The formation of Fe-rich saponite by the hydrothermal reaction of the hisingerite material is in agreement with the clay mineralogy of the underlying, deuterically altered green basalt. Electron microprobe analyses of the trioctahedral, saponitic clay minerals in one locality of the green basalt yielded an average composition (41 analyses) of $Na_{0.2}K_{0.05}Ca_{0.09}(Si_{6.37}Al_{1.30} \cdot Fe^{3+}{}_{0.33})(Fe^{3+}{}_{1.8}Mn_{0.02}Mg_{3.88})O_{20}(OH)_4$, similar to the formula listed in Table 2, if all Fe is taken as Fe^{3+}. Both formulae differ, however, from the average electron microprobe composition (10 analyses) of the nontronite (purified by DCB treatment) in the joints of the green basalt, $Na_{1.49}K_{0.01}(Si_{7.73}Al_{0.10}Fe^{3+}{}_{0.17})(Fe^{3+}{}_{2.90} \cdot Mn_{0.01}Mg_{1.03})O_{20}(OH)_4$. The nontronite is a dioctahedral, Mg- and Al-poor mineral. A detailed clay mineralogy of the green basalt will be reported elsewhere.

Although the composition of the trioctahedral smectite produced by the hydrothermal reaction of the unaltered grey basalt could not be determined due to the presence of feldspar and pyroxene, the smectite is likely an Fe-rich saponite, because it probably formed from the olivine (and glass) in the basalt, similar to the Fe-rich saponite in the matrix of the underlying green basalt, which is, in turn, similar in composition and XRD pattern to that produced by the hydrothermal treatment of hisingerite. Based on these results the hisingerite material may have the same origin as the interstitial glass and olivine, which have altered to the clay component of the green basalt and which formed a trioctahedral smectite during the hydrothermal treatment of the grey basalt. The Fe-rich saponite in the green basalt probably formed because the rock reacted with the steam that was generated from the river bed into which the basalt flowed. Because the hisingerite material had formed above the layer of basalt that reacted with the steam, it remained unaltered.

The formation of nontronite in the joints of the green basalt is difficult to explain. Papavassiliou and Cosgrove (1981) stated that after a high-temperature alteration of basalt, characterized by increase in Mg and loss in Ca and Fe^{2+}, subsequent low-temperature alteration results in losses of Mg, Ca, Fe^{2+}, and Na. Thus, although the material in the joints of the green basalt could have originally been Fe-rich saponite, considerable Mg may have been lost due to circulation of cold ground water through the joints, a fluctuation of the water table, or oxidation and reduction processes and converted the Fe-rich saponite to nontronite. The fact that goethite, rather than hematite, coexists with nontronite further indicates a low-temperature alteration. Shayan and Lancucki (1984) found that the ground water moving through the green basalt at Geelong had the composition (mmole/liter) of Na (88.8), Mg (8.5), Ca (0.85), Sr (0.01), CO_3^{2-} (1.2), HCO_3^- (11.2), SO_4^{2-} (3.94), and Cl^- (86.0) and a pH of 8.34. This composition may have been reached by river water moving through the surrounding Tertiary marine deposits before it intersected the basalt flow. A solution of similar composition, which would be capable of ionic exchange with the solids, may have been involved in low-temperature alteration of the green basalt near Geelong. Rock surfaces exposed in the joints and joint-material was probably more strongly influenced by such low-temperature alterations than the whole rock mass. Papavassiliou and Cosgrove (1981) proposed that low-temperature alteration superimposed on a high-temperature alteration produced Fe oxyhydroxides and Fe^{3+}-rich smectite.

The formation of Fe-rich saponite from hisingerite material appears to have involved the release of Fe from the hisingerite structure as a first step. At 340° and 370°C hematite was formed in the laboratory after 1 day of reaction, without the formation of clay. After 1 week, more hematite formed together with highly crystalline Fe-rich saponite. A temperature >180°C (probably closer to 340°C) appears to have been needed for the formation of the later, because no ordered clay mineral formed in the laboratory after 6 weeks of treatment at 180°C and after 445 days of treatment at 110°C.

Harder (1977) synthesized, in a few weeks to a few

https://doi.org/10.1346/CCMN.1988.0360406 Published online by Cambridge University Press

months, various smectites at room temperature (20°C) from solutions containing <60 ppm Si and 1–2.5 ppm of various metal cations, under alkaline to neutral pH conditions. He concluded that conditions similar to those in the experimental work were prevalent during lateritic weathering. Although such a process could have contributed to some extent to the formation of smectite in the joints of the green basalt, the initial deuteric alteration appears to have been dominant, as is evident from the fact that 20–40% smectite formed throughout the mass of the green basalt, as found by point counting microscopy (Cole *et al.,* 1984). Further work is in progress to compare the synthetic and natural formation of clay minerals in these basalts.

ACKNOWLEDGMENTS

The authors thank John Hamilton of the CSIRO Division of Mineral Chemistry for thermal analyses and Tony Turney of the Division of Materials Science and Geoff Taylor of Monash University for the hydrothermal runs. They also thank Alf Hohmann of Monash University for access to the electron microprobe and F. A. Mumpton for his constructive criticisms during the preparation of the manuscript.

REFERENCES

Bain, D. C., Ritchie, P. F. S., Clark, D. R., and Duthie, D. M. L. (1980) Geochemistry and mineralogy of weathered basalt from Morvern, Scotland: *Mineral. Mag.* **43,** 865–872.

Bain, D. C. and Russell, J. D. (1980) Swelling minerals in basalts and its weathering products from Morvern, Scotland: I. Interstratified montmorillonite-vermiculite: *Clay Miner.* **15,** 445–451.

Bain, D. C. and Russell, J. D. (1981) Swelling minerals in basalt and its weathering products from Morvern, Scotland: II. Swelling chlorite: *Clay Miner.* **16,** 203–212.

Bischoff, J. L. and Dickson, F. W. (1975) Seawater-basalt interaction at 200°C and 500 bars: Implications for origin of sea-floor heavy-metal deposits and regulation of seawater chemistry: *Earth Planet. Sci. Lett.* **25,** 285–397.

Brindley, G. W. (1972) Chlorite minerals: in *X-ray Identification and Crystal Structures of Clay Minerals,* G. Brown, ed., Mineralogical Society, London, 242–297.

Cole, W. F. and Lancucki, C. J. (1976) Clay minerals developed by deuteric alteration of basalt: in *Proc. Int. Clay Conf., Mexico City, 1975,* S. W. Bailey, ed., Applied Publ., Wilmette, Illinois, 35–43.

Cole, W. F., Lancucki, C. J., and Shayan, A. (1984) Verifying quarry potential: in *Proc. 12th Aust. Road Res. Board Conf. Vol. 12, Part 2, Hobart, 1984,* Australian Road Research Board, Vermont South, Victoria, 98–102.

Coulson, A. (1977) Age-relationships of Newer Basalts in the Geelong district, Victoria. *Proc. Royal Soc. Victoria* **89,** 159–165.

Cowking, A., Wilson, M. J., Tait, J. M., and Robertson, R. H. S. (1983) Structure and swelling of fibrous and granular saponitic clay from Orrock Quarry, Fife, Scotland: *Clay Miner.* **18,** 49–64.

Eggleton, R. A., Foudoulis, C., and Varkevisser, D. (1987) Weathering of basalt: Changes in rock chemistry and mineralogy. *Clays & Clay Minerals* **35,** 161–169.

Hajash, A. (1975) Hydrothermal processes along mid-ocean ridges: An experimental investigation: *Contrib. Mineral. Petrol.* **53,** 205–226.

Harder, H. (1977) Clay mineral formation under lateritic weathering conditions: *Clay Miner.* **12,** 281–288.

Kohyama, N., Shimoda, S., and Sudo, T. (1973) Iron-rich saponite (ferrous and ferric forms): *Clays & Clay Minerals* **21,** 229–237.

Luke, K., Taylor, H. F. W., and Kalousek, G. L. (1981) Some factors affecting formation of truscottite and xonotlite at 300°–350°C: *Cem. Conc. Res.* **11,** 197–203.

Mehra, O. P. and Jackson, M. L. (1960) Iron oxide removal from soils and clays by a dithionite-citrate system buffered with sodium bicarbonate: in *Clays and Clay Minerals, Proc. 7th Natl. Conf., Washington, D.C., 1958,* Ada Swineford, ed., Pergamon Press, New York, 317–327.

Mottl, M. J. and Holland, H. D. (1978) Chemical exchange during hydrothermal alteration of basalt by seawater: I. Experimental results for major and minor components of seawater: *Geochim. Cosmochim. Acta* **42,** 1103–1115.

Noack, Y., Emmermann, R., and Hubberten, H. W. (1979) Alteration in site 501 (leg 68) and site 504 (leg 69) basalts: Preliminary results: in *Initial Reports of the Deep Sea Drilling Project, Leg 69,* J. R. Cann, M. G. Langseth, J. Honnorez, R. P. von Horzen, S. M. White, *et al.,* eds., U.S. Government Printing Office, Washington, D.C., 497–508.

Papavassiliou, C. Th. and Cosgrove, M. E. (1981) Chemical and mineralogical changes during basalt-seawater interactions: Site 223, leg 23, D.S.D.P., north-west Indian Ocean: *Mineral. Mag.* **44,** 141–146.

Post, J. L. (1984) Saponite from near Ballarat, California: *Clays & Clay Minerals* **32,** 147–153.

Russell, J. D., Goodman, B. A., and Fraser, A. R. (1979) Infrared and Mössbauer studies of reduced nontronite: *Clays & Clay Minerals* **27,** 63–71.

Scheidegger, K. F. and Stakes, D. S. (1977) Mineralogy, chemistry and crystallization sequence of clay minerals in altered tholeiitic basalts from the Peru trench: *Earth Planet. Sci. Lett.* **36,** 413–422.

Scott, R. B. and Hajash, Jr., A. (1976) Initial submarine alteration of basaltic pillow lavas: A microprobe study: *Amer. J. Sci.* **276,** 480–501.

Senkayi, A. L., Dixon, J. B., Hassner, L. R., and Viani, B. E. (1983) Mineralogical transformation during weathering of lignite overburden in East Texas: *Clays & Clay Minerals* **31,** 49–56.

Seyfried, W. E., Jr. and Bischoff, J. L. (1979) Low temperature basalt alteration by seawater: An experimental study at 70°C and 150°C: *Geochim. Cosmochim. Acta* **43,** 1937–1947.

Seyfried, W. E., Jr., and Bischoff, J. L. (1981) Experimental seawater-basalt interaction at 300°C, 500 bars, chemical exchange, secondary mineral formation and implications for the transport of heavy metals: *Geochim. Cosmochim. Acta* **45,** 135–147.

Seyfried, W. E., Shanks, W. C., and Bischoff, J. L. (1976) Alteration and vein formation in site 321 basalts: in *Initial Reports of the Deep Sea Drilling Project, Leg 34,* R. S. Yeats, S. R. Hart, *et al.,* eds., U.S. Government Printing Office, Washington, D.C., 385–392.

Shayan, A. (1984) Hisingerite material from a basalt quarry near Geelong, Victoria, Australia: *Clays & Clay Minerals* **32,** 272–278.

Shayan, A. and Lancucki, C. J. (1984) Konyaite in salt efflorescence from a Tertiary marine deposit near Geelong, Victoria, Australia: *Soil Sci. Soc. Amer. J.* **48,** 939–942.

Stevula, L. and Petrovic, J. (1983) Formation of an inter-

https://doi.org/10.1346/CCMN.1988.0360406 Published online by Cambridge University Press

mediate C-S-H phase during the hydrothermal synthesis of gyrolite: *Cem. Conc. Res.* **13,** 684–688.

Stucki, J. W., Golden, D. C., and Roth, C. B. (1984) Preparation and handling of dithionite-reduced smectite suspensions: *Clays & Clay Minerals* **32,** 191–197.

Van der Marel, H. W. and Beutelspacher, H. (1976) *Atlas of Infrared Spectroscopy of Clay Minerals and their Admixtures:* Elsevier, Amsterdam, pp. 144, 148, 200, 204, 322.

Walters, S. G. and Ineson, P. R. (1983) Clay minerals in the basalts of the South Pennines: *Mineral. Mag.* **47,** 21–26.

(Received 2 May 1987; accepted 8 February 1988; Ms. 1669)

https://doi.org/10.1346/CCMN.1988.0360406 Published online by Cambridge University Press